Electrical and thermal properties of fluorine-intercalated graphite fibers

L. Piraux, V. Bayot, and J. P. Issi
Unité de Physico-Chimie et de Physique des Matériaux, Département des Sciences des Matériaux et des Procédés, Université Catholique de Louvain, place Croix de Sud 1, B-1348 Louvain-la-Neuve, Belgium

M. S. Dresselhaus
Department of Electrical Engineering and Computer Science and Department of Physics, Massachusetts Institute of Technology, Cambridge, Massachusetts 02139

M. Endo
Department of Electrical Engineering, Faculty of Engineering, Shinshu University, Nagano 380, Japan

T. Nakajima
Division of Molecular Engineering, Graduate School of Engineering, Kyoto University, Sakyo-ku, Kyoto 606, Japan
(Received 27 September 1989)

We report measurements on the electrical- and thermal-transport properties of fluorine-intercalated vapor-grown carbon fibers C_xF with the carbon-to-fluorine-atom ratio x between 4.1 and 5.8. The electrical resistivity is found to be very sensitive to the fluorine concentration. Indeed, while the resistivities of the $C_{5.2}F$ and the $C_{5.8}F$ compounds are well below that of the pristine graphite fibers, the tendency is reversed when $x \leq 4.5$ and large resistivity values are obtained. All C_xF compounds exhibit a logarithmic resistance increase at low temperature, which can consistently be explained by weak-localization and carrier-carrier interaction effects for two-dimensional electron systems. Large negative magnetoresistance values have been measured on the C_xF compound with $x = 4.1$. At higher temperature, an anomalous resistance-versus-temperature behavior appears for each fluorine-intercalated vapor-grown carbon fiber, possibly resulting from a phase transition. Heat transport in C_xF (with $x = 4.1$) is almost entirely governed by lattice vibrations between 2.5 and 300 K while the thermoelectric power is positive, and its temperature dependence is similar to that previously observed in other acceptor graphite intercalation compounds. Our results indicate that the high resistivity of the C_xF compounds (with $x \leq 4.5$) is due to strong defect scattering rather than a low free-charge-carrier density.

I. INTRODUCTION

For most graphite intercalation compounds, an increase in the intercalate concentration leads to an increase in carrier concentration and in the electrical conductivity up to some optimal intercalate concentration y_c. And so also is the case for the ionic fluorine intercalation compounds based on a variety of graphite host materials: single-crystal flakes, highly oriented pyrolytic graphite (HOPG),[1] graphite powder,[2] and vapor-grown carbon fibers (VGCF).[3,4] For typical graphite acceptor intercalation compounds, further increase in intercalate concentration beyond y_c results in a decrease in σ, but by a small amount,[5] on the order of a factor of perhaps 2. This effect is explained by a decrease in the carrier mobility that is more rapid than the increase in carrier concentration as the intercalate concentration increases beyond y_c. The situation for the ionic fluorine compounds is unusual insofar as the decrease in σ from $\sigma(y_c)$ can be greater than an order of magnitude by the time a stage-1 compound is reached. It should be further noted that for the ionic fluorine compounds, stage 2 corresponds to a range of fluorine-concentration values, as is also the case for stage-1 compounds,[1,3] and for this reason the stoichiometric designation is of particular importance for the specification of the ionic fluorine compounds. A second unusual feature is the ability of fluorine to form both covalent and ionic graphite compounds.[2] The anomalous behavior of the low-stage fluorine compounds has been attributed to the presence of some covalent bonding in the otherwise ionic compound.[2,6]

In this paper we show that the order-of-magnitude decrease in σ from its maximum value $\sigma(y_c)$ leads to a favorable situation for exploring new regimes in the electrical- and thermal-transport properties of solids. Furthermore, the fiber geometry is found to be especially favorable for the study of these phenomena. Specifically, we address in this paper an anomalous behavior in the electrical resistivity and magnetoresistance, as well as in the thermal conductivity and thermopower, all arising from the large decrease in carrier mobility as the carbon-to-fluorine-atom ratio decreases beyond 4.5. Furthermore, study of a variety of transport properties of a C_xF fiber in the low limit of x values used in the present study ($4.1 \leq x \leq 5.8$) provides new insight into the mechanism responsible for the large decrease in σ relative to $\sigma(y_c)$. We begin with an overview of the anomalous transport phenomena that are encountered, then proceed to present

our detailed results for each of the electrical- and thermal-transport properties and finally we discuss the underlying physics that interrelates all these phenomena.

With regard to the resistivity, we confirm for the first time the anomalous low conductivity (high resistance) of a high-fluorine-concentration graphite intercalation compound in a fibrous host material. Below a carbon-to-fluorine-atom ratio $x=4.5$, the resistivity exhibits a strong increase in magnitude, in agreement with previous results obtained on HOPG-fluorine intercalation compounds.[1] By carrying out a detailed study of the temperature dependence of the electrical resistivity, two anomalous regimes are identified. In the low-temperature limit, the electrical resistivity is dominated by an extremely large logarithmic increase in resistance, greater by an order of magnitude than that previously observed in any graphite-based system,[7,8] thereby allowing study of this phenomenon on a level of detail that was not previously possible. Similarly, the anomalous behavior near ~ 170 K is especially pronounced in highly concentrated fluorine graphite fibers and is suggestive of a structural phase transition. The good resolution of the resistivity measurements allows a clear identification of the temperature range where detailed structural studies should be carried out.

The magnetoresistance studies likewise give additional information. Whereas the pristine vapor-grown fibers of the present study exhibit a positive magnetoresistance, the C_xF intercalated fibers studied here in detail show a negative magnetoresistance over the entire temperature range where magnetoresistance effects are seen. This observation implies that the negative magnetoresistance of intercalated fibers cannot be explained by the presence of unintercalated regions, as had been previously proposed,[9,10] but rather is a phenomenon to be explained in its own right. In the present paper, the magnetoresistance measurements are interpreted in terms of elastic- and inelastic-scattering processes and are used to separate the carrier localization effect from the carrier-carrier Coulomb interaction effect, following previous works[7,8] on samples showing similar functional behavior but an order of magnitude smaller in size. The very low magnitude of the magnetoresistance above 100 K provides support for the relatively low mobility of carriers in this compound and is consistent with the failure to observe magneto-oscillatory (Shubnikov–de Haas) effects in the low-temperature magnetoresistance.[11]

Likewise, the thermal-transport phenomena observed in the same C_xF intercalated fibers as were used for the electrical-transport studies is unusual for acceptor intercalation compounds. The thermal conductivity for graphite acceptor intercalation compounds normally exhibits an important contribution at low temperatures from the charged carriers. However, in this high-fluorine-concentration graphite intercalation compound, the magnitude of the electronic thermal conductivity is exceptionally low for an acceptor graphite intercalation compound (GIC) and essentially all the heat is carried by phonons, even at low temperatures. More detailed study of the thermal-transport phenomenon is therefore likely to provide further information on the dominant scattering processes in the various temperature regimes and on the low-temperature lattice thermal conductivity enhancement associated with the intercalate and reported in a previous work.[12]

Finally, the temperature dependence of the thermopower provides additional information about the carriers and their interaction with the lattice. The positive sign of the thermopower and the general features of its temperature dependence (a linear dependence at low temperature and a broad maximum at elevated temperature) are normal for acceptor GIC's. From the results obtained in the low-temperature range, estimations are made of the Fermi energy as well as of the carrier density.

In Sec. II, we present a description of the sample preparation and characterization, while Sec. III describes the experimental setup for the measurements. The results are presented and discussed in Sec. IV for the resistivity, in Sec. V for the magnetoresistance, and in Sec. VI for the thermal conductivity and the thermopower. Finally, in Sec. VII, we present our conclusions.

II. PREPARATION AND COMPOSITION OF C_xF

Vapor-grown carbon fibers (VGCF), heat treated to $T_{HT}=2950\,^{\circ}C$, and having a weight of 0.04–0.05 g were closely packed with Ag-metal powder (0.25 g) in a Ni vessel, which was then placed in a Ni reactor without using a water cooling jacket. The temperature of the reactor was gradually increased to 200 °C under high vacuum, which was attained by rotary and diffusion pumps. Fluorine gas (Daikin Kogyo Company, Ltd., with a purity of F_2: 99.4–99.7 %, N_2: 0.3–0.6 %, HF $<0.01\%$) was introduced into the reactor to 1 atm, and after 10–20 min, the reactor was evacuated again by a rotary pump followed by a diffusion pump. This operation was repeated five times during a period of three days to remove any residual HF in the reactor. This HF is generated by the reaction of fluorine gas with water adsorbed on the walls of the reactor vessel and on the raw materials. The trace level of HF in the fluorine gas was checked to be $\leq 0.01\%$ by ir spectroscopy during an experimental run using an ir cell with a CaF_2 window which was closely connected to the reactor. The temperature of the reactor was maintained at 200 °C for one day to fluorinate Ag metal to silver fluoride, and then the reactor was cooled to room temperature. The fluorine-gas pressure was adjusted to 1 atm after cooling the reactor. After 8–18 days, the fluorine gas was replaced by nitrogen gas, and the final C_xF sample was obtained.

The composition of each sample was determined by weight uptake, and the stage number and repeat distance along the c axis (I_c) were found by x-ray diffraction (see Table I). The C_xF fiber samples used for most of the transport-properties measurements reported here exhibited an x-ray-diffraction pattern for a stage-1 compound with an I_c value of 5.18 Å. A very strong (001) diffraction line was observed with a very weak (002) line in the quasi-first-stage $C_{4.1}F$ sample. In general, the $(00n+1)$ line (where n is the stage number) is strongest when an intercalated layer is situated at the center of two

TABLE I. Sample characteristics for C_xF fibers.

Sample	x	Stage	I_c (Å)	Reaction time (days)
1	4.1	1st + small amount of 2nd	5.18 (1st) 9.42 (2nd)	18
2	4.5	1st + small amount of 2nd	5.16 (1st) 9.53 (2nd)	34
3	5.2	2nd + small amount of 1st	9.38 (2nd) 5.12 (1st)	14
4	5.8	2nd	9.29	7

carbon sheets. But the intensity of the $(0\,0\,n)$ line increases as the position of the fluorine atom deviates somewhat above or below the center of the two surrounding carbon sheets due to an increase in the chemical bonding between the carbon and fluorine. According to the charge transfer, the chemical bond between carbon and fluorine varies from ionic to semi-ionic in character.[13,14]

With regard to the stoichiometry, a trace amount of Ag was detected in the C_xF samples by atomic-absorption spectra, and diffraction lines associated with AgF were sometimes found in the x-ray-diffraction spectra of the C_xF fibers. It is known that a small amount of fluoride such as HF, AsF_5 IF_5, LiF, AlF_3, or AgF assists the intercalation of fluorine into graphite.[2,13–17] Specifically, a highly oxidized silver fluoride AgF_x could facilitate fluorine intercalation around the graphite surface in accordance with the room-temperature reaction.

III. EXPERIMENTAL SETUP

The electrical resistivity was measured on individual fiber samples between 1.5 and 300 K by means of a classical four-probe dc method. For each sample, the input power was kept below 10^{-6} W to avoid self-heating, and the resistance measurements were performed with an accuracy of one part in 10^5. Magnetic fields up to 1 tesla were provided by means of a simple electromagnet. The C_xF fiber sample (see sample 3 in Table I) was mounted with the fiber axis perpendicular to the applied magnetic field, and reliable electrical contacts were made using platinum paste.

Thermal conductivity and thermoelectric-power measurements were performed using a sample holder specially designed to measure samples of extremely small cross section. The experimental arrangement, which is based on the principle of a four-probe thermal potentiometer, is described in detail elsewhere.[18] The sample used for the thermal-conductivity measurements consisted of a bundle of five fibers in order to increase the sample heat conductance relative to the heat losses. A prior calibration of the system allowed estimation of the heat losses by radiation in the temperature range range 100–300 K while the voltage probes for the thermoelectric-power measurements were previously calibrated below 90 K using a superconducting Y-Ba-Cu-O ceramic sample.

IV. ANALYSIS OF THE EXPERIMENTAL RESULTS OBTAINED AT ZERO MAGNETIC FIELD

In this section, we discuss the electrical-resistivity results obtained on fiber samples with different fluorine concentrations. From Fig. 1, we see that both the magni-

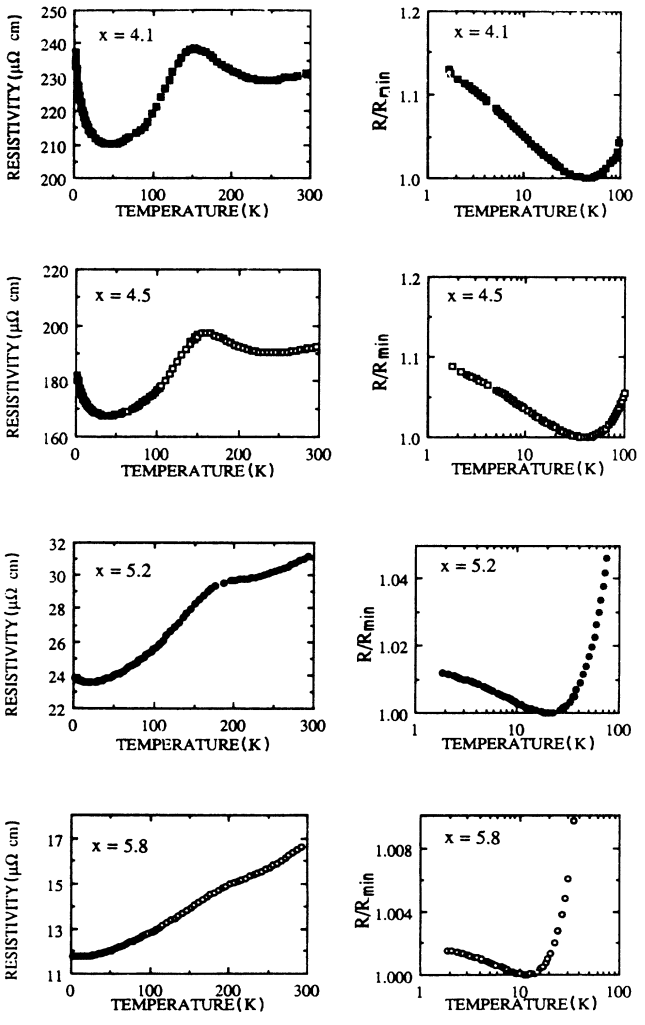

FIG. 1. Temperature dependence of the resistance for C_xF samples (with $x = 4.1$, 4.5, 5.2, and 5.8) using a linear and a logarithmic temperature scale. For the log plots, the measured resistance is normalized to the resistivity minimum.

TABLE II. Summary of transport measurements on C_xF fibers. The asterisk denotes results from Ref. 3.

Sample	x	$\rho_{300\text{ K}}$ ($\mu\Omega$ cm)	$\rho_{4.2\text{ K}}$ ($\mu\Omega$ cm)	$(\Delta R/R)_{\text{decade}}$ (10^{-2})	$\alpha p+\gamma$
1*A*	4.1	230	230	9.6	0.76
1*B*	4.1	250	229	7.7	0.61
1*C*	4.1	272	280	9.3	0.60
2	4.5	195	178	7.1	0.72
3	5.2	31	24	1.2	1.65
4*A*	5.8	40	29	0.45	0.51
4*B*	5.8	17	12	0.28	0.76
5*	10.8	20	13.4		

tude of the resistivity values and the shape of the $\rho(T)$ curves drastically change with fluorine concentration. For the C_xF fiber samples of high fluorine concentration (samples 1 and 2 in Table I), the resistivity is much higher than that of pristine fibers, while for the lower fluorine concentration fibers (samples 3 and 4 in Table I) the situation is reversed. Indeed, the resistivity of a pristine VCGF heat treated at around 2950 °C is typically 80 $\mu\Omega$ cm.[19] This evolution of the resistivity values versus fluorine concentration is quite similar to that obtained previously on HOPG-fluorine GIC's.[1] With regard to the high-fluorine-concentration compounds (samples 1 and 2), we observe a strong logarithmic increase of resistivity with decreasing temperature at low temperature, while a strong anomaly appears near 170 K, as previously observed in measurements of the resistivity $\rho(T)$ (Ref. 3) and of the *c*-axis thermal expansion and the nuclear magnetic resonance (NMR) linewidth,[20] and tentatively attributed to a structural phase transition. The resistance rise below 50 K is larger by an order of magnitude than previously observed manifestations of this logarithmic dependence effect in $\rho(T)$ in other GIC's.[7,8] Furthermore, the temperature at which the resistance minimum occurs (40 K) is also higher relative to that for other acceptor-intercalated carbon fibers previously investigated (2–27 K).[7,8]

For the C_xF compounds with lower F concentrations (samples 3 and 4 in Table I), both the high-temperature anomaly and the low-temperature logarithmic behavior are considerably reduced, as seen in Fig. 1. The anomalous inflection observed around 190 K for the sample 4 (where $x=5.8$) is quite similar to that previously reported on a $C_{10.8}F$ sample.[3] The logarithmic increase of resistivity observed in the low-temperature range is more than 1 order of magnitude lower than that observed on the high F concentration (samples 1 and 2 of Table I). With regard to both anomalies observed at low temperatures and around 170–200 K, it is difficult to make a comparison of the present work on graphite fibers with previous transport measurements for HOPG-based F GIC's.[1] Indeed, the in-plane resistivity measurements of the HOPG-based samples were made using an ac technique of much lower resolution and they were not extended below 50 K.

We identify two mechanisms to be responsible for the logarithmic anomaly: a single-carrier weak localization effect produced by constructive quantum interferences between elastically backscattered partial carrier waves,[21,22] and charge-carrier many-body Coulomb interactions.[23,24] Both effects are enhanced in the presence of disorder, i.e., defect scattering. Theoretical considerations have shown that the magnetoresistance at small magnetic fields can be used to separate the weak-localization contribution from the electron-electron interactions contribution.[23]

In the two-dimensional regime, the logarithmic variation of the resistance over a decade of temperature, due to the occurrence of both weak-localization and Coulomb-interaction effects, is given by

$$\left[\frac{\delta R}{R}\right]_{\text{decade}}=(2.84\times10^{-5})R_{\square}(\alpha p+\gamma)\ , \tag{1}$$

where $R_{\square}$ is the resistance per square, i.e., the measured resistivity of the sample divided by the *c*-axis repeat distance I_c.[7] The weak-localization contribution is determined by the product αp, where p is the exponent in the temperature dependence of the inverse of the inelastic scattering time ($1/\tau_i \propto T^p$) and where the value of α depends on the effect of spin-dependent processes due to magnetic scattering and spin-orbit coupling. The Coulomb interaction contribution is given by γ, where γ (which is a measure of the screening by other charge carriers) has a value close to 1 in the limit of weak screening.[23] As is the case for the electrical resistivity, the strength of the weak-localization and Coulomb-interaction effects is very sensitive to the carbon-to-fluorine concentration. Table II summarizes the values of the electrical parameters of selected samples.

V. ANALYSIS OF THE EXPERIMENTAL RESULTS OBTAINED IN A TRANSVERSE MAGNETIC FIELD

In this section, we analyze in detail the transverse magnetoresistance results obtained on our highest F concentration fiber sample (sample 1 of Table I). Detailed analysis of the magnetoresistance curves as a function of temperature and magnetic field using weak-localization theoretical relations allows us to obtain reliable data for the different phase-breaking scattering times, i.e., the inelastic scattering time τ_i, the magnetic scattering time τ_s, and the spin-orbit scattering time $\tau_{\text{s.o.}}$. Indeed, an exter-

nal transverse magnetic field quenches the weak-localization effect when the magnetic field becomes greater than

$$H_k = \frac{\hbar}{4eD\tau_k} , \tag{2}$$

where $k = i, s$, s.o. labels the different scattering processes listed above, and $D = (v_F^2 \tau_0)/2$ is the two dimensional (2D) diffusion constant. In particular, for a magnetic field H much larger than the inelastic characteristic magnetic field H_i, the logarithmic increase of the resistance due to weak localization is suppressed. The very high anisotropy of the electrical conductivity ($\sigma_a/\sigma_c = 10^6$) of the fluorine graphite intercalation compounds[1] allows us to consider the charge-carrier system as a quasi-2D hole gas. The magnetoresistance arising from 2D weak-localization effects, in which the magnetic field H is oriented perpendicular to the 2D carrier system, is expressed as[22]

$$\frac{\Delta R(H,T)}{R(0,T)} = -\frac{e^2}{2\pi^2\hbar}\lambda R_\square \left[\tfrac{1}{2}\Psi\left(\frac{1}{2}+\frac{H_1(T)}{H}\right) - \tfrac{1}{2}\Psi\left(\frac{1}{2}+\frac{H_2(T)}{H}\right) - \ln\left(\frac{H_1^{3/2}}{H_2^{1/2}H}\right)\right] , \tag{3}$$

where $\Delta R(H,T) = R(H,T) - R(0,T)$, and Ψ is the digamma function. The dimensionless factor λ should be unity for perfectly homogeneous systems.[25] Also we use $H_1(T)$ and $H_2(T)$ to denote

$$H_1(T) = H_i(T) + \tfrac{4}{3}H_{\text{s.o.}} + \tfrac{2}{3}H_s ,$$

$$H_2(T) = H_i(T) + 2H_s . \tag{4}$$

For the case of a fiber, a comparison between the experimental results and theory requires the integration of the magnetoresistance over the assumed isotropic distribution of the cross-sectional graphite-layer arrangement in the fiber. Therefore, the apparent magnetoresistance, i.e., the experimental magnetoresistance $[\Delta R(H,T)/R(0,T)]_{\text{expt}}$ is given by[8]

$$\left[\frac{\Delta R(H,T)}{R(0,T)}\right]_{\text{expt}} = \frac{1}{\pi}\int_{-\pi/2}^{\pi/2}\left[\frac{\Delta R(H\cos\theta,T)}{R(0,T)}\right]_{\text{theor}} d\theta , \tag{5}$$

where θ is the angle between the normal to a graphite layer and the magnetic field direction. The theoretical magnetoresistance which appears under the integral is the one that would be observed if the magnetic field were perpendicular to each graphite layer.

We now consider the magnetoresistance results and compare them to the above-mentioned theories. In Fig. 2, we present magnetoresistance curves obtained from a C_xF fiber sample 1 of Table I at different temperatures and as a function of a magnetic field perpendicular to the fiber axis. It is seen that the magnetoresistance is negative and that its magnitude increases with decreasing temperature. These features are consistent with the weak-localization effect. Moreover, this result indicates that the negative magnetoresistance does not originate from unintercalated regions as previously suggested,[9,10] since the pristine VGCF heat treated at 2950 °C do not exhibit negative magnetoresistance at any of the temperatures considered in Fig. 2. Above 100 K, the magnetoresistance of the fluorine intercalated fibers becomes nearly negligible. In particular, no apparent magnetoresistance anomaly was detected near 170 K.

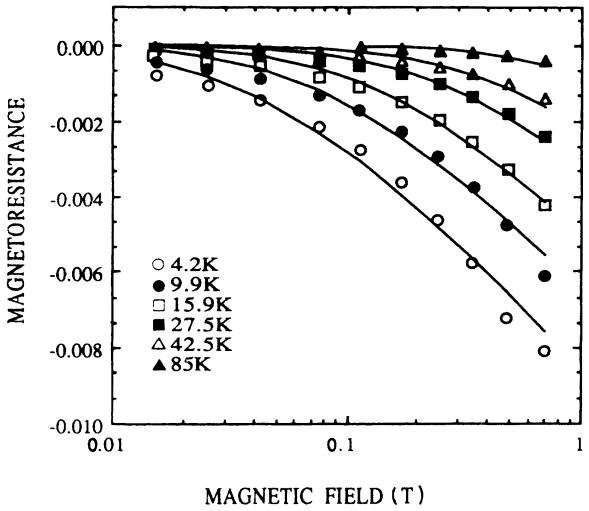

FIG. 2. Transverse negative magnetoresistance vs magnetic field for a C_xF fiber sample ($x = 4.1$) at various temperatures, as indicated. The solid lines are calculated from a best fit using the weak-localization theory [relations (3), (4) and (5)].

Next, we analyze these curves in detail using the weak-localization relation (3). Since at low temperature no positive magnetoresistance appears in the low-magnetic-field range, spin-orbit coupling is negligible in our sample. So, in the fitting procedure, we set $H_{\text{s.o.}} \ll H_i, H_s$ at each temperature. There are then three fitting parameters H_i, H_s, and λ for the theoretical formula of the magnetoresistance. Among these, H_i is temperature dependent, while the two parameters H_s and λ are independent of temperature. The weak-localization relations, containing these three adjustable parameters, are introduced under the integral in Eq. (5) in order to take into account the orientation of the graphite layers in the fiber with respect to the magnetic field.

The solid lines of Fig. 2 represent the best fits to the negative magnetoresistance at various temperatures and over a wide magnetic field range for the fluorine intercalated graphite fiber sample. The good fit that is obtained provides quite convincing evidence for the interpretation, since the model accounts for both the temperature and magnetic field dependences of the negative magnetoresistance very well. From the fit, λ takes the value of 0.1, while H_s is very small (less than 10^{-4} tesla). The temperature-dependent parameter H_i related to inelastic scattering can be accounted for by an expression of the

form $H_i=\alpha' T+\beta' T^2$ with $\alpha'=0.85\times10^{-3}$ T/K and $\beta'=1.4\times10^{-5}$ T/K^2. Since the ratio $\alpha'/\beta'\sim60$, a linear temperature dependence dominates H_i at low temperature, and a quadratic law at high temperature. We note that H_s is much smaller than H_i above 1 K so that the dominant phase coherence breaking mechanism is inelastic scattering by holes and phonons.

The temperature dependence of H_i between 3 K and 100 K is shown in Fig. 3. Using relation (2) it is possible in principle to estimate the values of the inelastic-scattering time τ_i at each temperature. However, one difficulty with doing so is that the electronic diffusion constant D is not well known, since D is a function of both v_F and τ_0, neither of which can be determined accurately. Nevertheless, a rough estimate of D can be obtained taking characteristic values for low-stage acceptor GIC's, $v_F\approx8\times10^5$ m/s and using $\tau_0=l_0/v_F$, where $l_0=\pi\hbar I_c/\rho_0 e^2 k_F$ is the charge-carrier mean free path deduced in the approximation of the 2D Blinowski-Rigaux band-structure model.[26] We thus find $l_0\approx15$ Å, $\tau_0\approx2\times10^{-15}$ s, and $D\approx6.5\times10^{-4}$ m^2/s. By comparison, the mean free path of a $C_{2.9}F$ HOPG-based sample[1] (with an in-plane resistivity of 400 $\mu\Omega$ cm) was estimated in a similar way between 4 and 10 Å. From this result, the authors conclude that the domain wall scattering mechanism does not govern the electrical conduction of the $C_{2.9}F$ HOPG-based sample. Using relation (2), we finally obtain $1/\tau_i=(3.5\times10^9)T+(5.5\times10^7)T^2$. In a previous paper,[8] we gave arguments to show that the linear term and the quadratic term were associated with carrier-carrier inelastic scattering and carrier-phonon inelastic scattering, respectively. Table III compares the weak-localization parameters for the C_xF fiber sample 1 of Table I to those for previous studies on metal chloride intercalated graphite fibers.[7–8] We also note that the

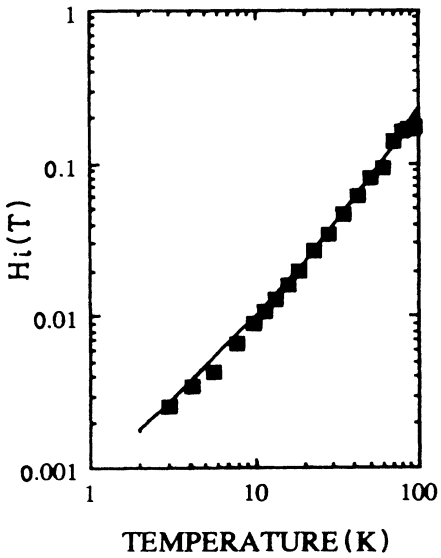

FIG. 3. Temperature dependence of the best fit values of H_i. The solid lines correspond to the fit using the $\alpha' T+\beta' T^2$ relation with $\alpha'=0.85\times10^{-3}$ T/K and $\beta'=1.4\times10^{-5}$ T/K^2, while the square symbols are the individually adjusted values of $H_i(T)$.

TABLE III. Parameters describing weak-localization behavior in intercalated graphite fibers. The asterisks denote coefficients in the relation $1/\tau_i=aT+bT^2$. The dagger denotes sample 1 of Table I.

	$\rho_{4.2\,K}$ ($\mu\Omega$ cm)	T_{min} (K)	$(\Delta R/R)_{decade}$ (10^{-2})	$k_F l_0$	D (10^{-3} m^2/s)	τ_i (10^{-11} s)	a^* (10^9/s K)	b^* (10^7/s K^2)
Fluorine intercalated graphite fiber (this work†)	230–280	37–45	7.7–9.6	3	0.65	>250	3.5	5.5
Previous studies on metal chloride intercalated graphite fibers (Refs. 7 and 8)	7–50	2–27	0.1–0.85	20–130	6–45	0.8–1.6	2.9–3.9	8.4–9.6

magnetic-scattering time τ_s is much larger in the fluorine compounds than in metal chlorides GIC's. This may be due to the fact that the host graphite materials are different in both studies (VGCF in the present work and pitch-based carbon fibers in the previous studies), since Fe catalyst particles are used in the preparation of VGCF.

In order to determine the relative importance of weak-localization and Coulomb-interaction contributions, we compare the temperature variation of the resistance in a transverse magnetic field with that obtained in zero magnetic field. Indeed, it is well known that a magnetic field applied perpendicular to the 2D charge-carrier system tends to destroy the weak-localization effect while the sensitivity of the Coulomb interaction to a small magnetic field is quite negligible.[23] Figure 4 shows the effect of a magnetic field on the rate of the logarithmic increase of resistance for one of the first-stage ionic fluorine graphite fiber intercalation compounds. We see that the rate decreases rapidly as a function of H for low magnetic field and then saturates above approximatively $H=0.4$ tesla. The remaining logarithmic resistance increase in the presence of a magnetic field of $H>0.4$ tesla is caused only by the carrier-carrier interaction effect. Since the magnetic field introduces only a little perturbation to the coefficient of the logarithmic variation (about 10%), it can be concluded that the logarithmic dependence of the resistivity is predominantly due to the carrier-carrier interaction effect.

Finally, we note that the above relations (2)–(4) describing the weak-localization phenomenon are only valid in the weak-disorder limit, i.e., when the product $k_F l_0$ (where k_F is the Fermi wave vector and l_0 is the carrier mean free path) is greater than unity. Taking the Fermi energy value $E_F=0.9$ eV as determined by optical reflectivity measurements[6] for the $C_{4.1}F$ compounds, we obtain $k_F=2\times10^9$ m^{-1} and $k_F l_0=3$ using the 2D Blinowski-Rigaux band-structure model. By contrast, for the previously studied low-stage acceptor GIC's,[7] $k_F l_0$ was in the range between 20 and 130. This result suggests that the synthesis of more concentrated fluorine intercalated VGCF of higher resistivity can lead to a product $k_F l$ smaller than unity. Indeed, optical-reflectivity data[6] revealed that the Fermi energy (and therefore also k_F) does not vary significantly with the fluorine concentration for $4<x<9$, while l_0 is expected to be drastically sensitive. So, we expect that fluorine-intercalated VGCF are very appropriate materials to study the transition between the weak-disorder regime and the strong-disorder regime for which the underlying physics for electronic conduction is quite different.

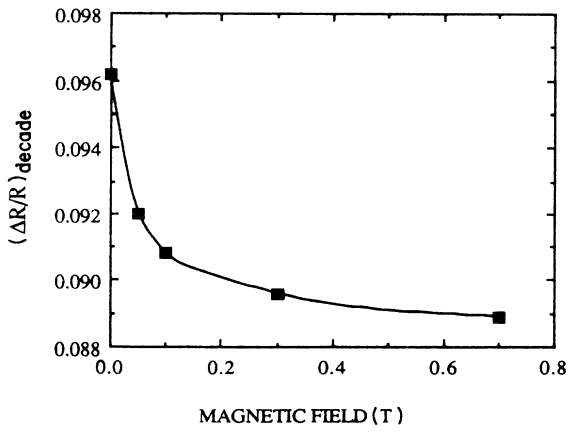

FIG. 4. Influence of a magnetic field on the variation of resistance over a decade of temperature $(\delta R/R)_{decade}$ for a fibrous C_xF sample ($x=4.1$). The square symbols are the experimental points obtained from the logarithmic temperature dependence of the resistance at various magnetic fields. The solid line is a guide for the eyes.

VI. THERMAL CONDUCTIVITY AND THERMOPOWER

Figure 5 shows the temperature dependence of the thermal conductivity from room temperature down to 2.5 K of a batch of five C_xF fibers taken from sample 1 of Table I. By contrast with other previously studied low stage acceptor GIC's, the electronic contribution to the thermal conductivity is negligible over the whole temperature range investigated. Indeed, the electronic thermal conductivity κ_E can be directly calculated from the electrical resistivity data via the Wiedemann-Franz law when elastic scattering dominates, which is certainly the case in the low-temperature range. This gives, at 4.2 K, $\kappa_E=0.05$ W m^{-1} K^{-1}, which is only one-tenth of the experimental thermal conductivity value. Above 50 K, the temperature dependence of the thermal conductivity is quite similar to that observed in pristine graphitic materials. The results of Fig. 5 allow us to estimate the phonon mean free path in the boundary scattering regime, applying the Kelly procedure for graphitic materials.[27] Taking the measured thermal conductivity value at 80 K, we find for our sample a phonon mean free path of about 250 Å,

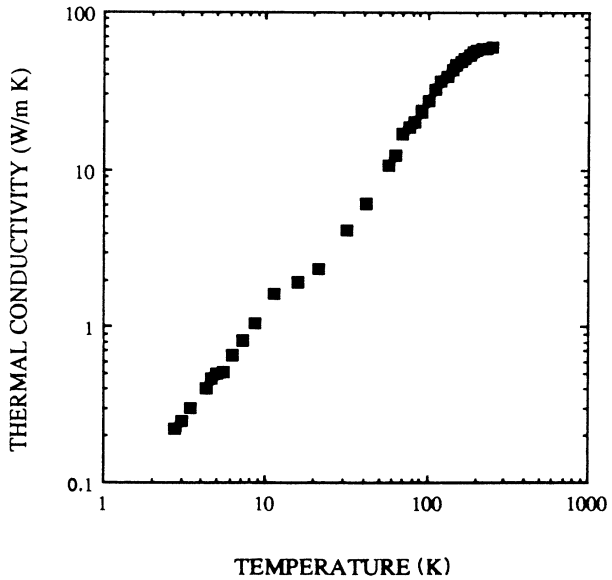

FIG. 5. Temperature variation of the thermal conductivity of a fibrous C_xF sample ($x=4.1$) presented on a log-log plot.

which is about a factor 3 lower than a previous estimate for the phonon mean free path of a low stage VGCF-$CuCl_2$ compound.[26] We also note that the hole mean free path is more than 1 order of magnitude lower than the phonon mean free path, while for the VGCF-$CuCl_2$ compound they were comparable.[26] In the low-temperature range, the temperature dependence in Fig. 5 deviates from the graphitic behavior, giving rise to a significant enhancement of the lattice thermal conductivity. Such behavior was previously observed in other acceptor GIC's (Ref.12) and results from a modification of the low-frequency phonon modes through introduction of phonon modes associated with the intercalate. Indeed, it was found that this additional low-temperature lattice contribution to the thermal conductivity decreases as the stage index increases.[12]

The temperature variation, from 2.5 to 300 K, of the thermoelectric-power $S(T)$ of the same C_xF fiber sample as in Fig. 5 is presented in Fig. 6. The temperature dependence of the thermopower is quite similar to that previously observed for other low-stage acceptor GIC's:[12,18–30] starting at low temperature, first we see an increase in S with temperature, followed by a broad maximum around 200 K. For the C_xF fiber sample in Fig. 6, it appears that the value of the thermoelectric power at the maximum (16 μV/K) is slightly lower than for other stage-2 acceptor GIC's ($S_{max}=20-30$ μV/K). In the low-temperature range, a quasilinear function of the temperature for $S(T)$ is observed. The coefficient of the linear variation of the thermoelectric power ($S/T=3.5\times10^{-8}$ V/K^2) is close to that previously obtained on a stage-2 HOPG-$SbCl_5$ sample.[29] Using relations for the diffusion thermoelectric power obtained within the framework of the Blinowski-Rigaux model, we can estimate the Fermi energy from the low-temperature variation of the thermoelectric power.[30] From such analysis, we obtain $E_F=0.9$ eV, in good agreement with the Fermi-energy values yielded by optical-reflectivity measurements[6] for a C_xF sample with $x=4.1$. This result suggests that the carrier density for a sample with $x=4.1$ is comparable to that in other low stage acceptor GIC's. We therefore conclude that the low hole mobility in the fluorine intercalation compounds is due to strong defect scattering, thereby giving rise to the high resistivity. The observation of a disorder-induced line in the Raman spectra of stage-2 $C_{6.4}F$ intercalated HOPG (Ref. 31) also confirms the importance of defect scattering.

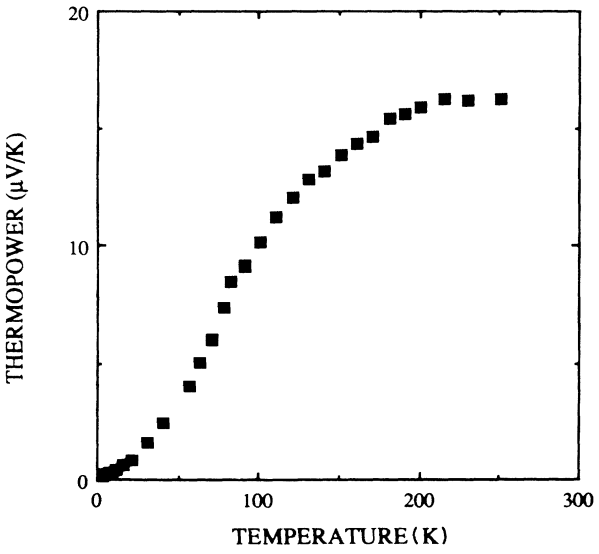

FIG. 6. Temperature dependence of the thermoelectric power of a fibrous C_xF sample ($x=4.1$).

Previous calculations have shown that the effects of both weak-localization and electron-electron interaction give rise to a logarithmic correction to the diffusion thermopower in the 2D limit.[32,33] In our case, however, it is difficult to verify these predictions experimentally, since the potentiometric method used in this experiment does not allow us to determine the thermoelectric power very accurately (the error is about 10% at low temperature). For the sample showing the largest effects, a resolution of at least 1% should be required to extract the expected logarithmic temperature-dependent term from the linear variation of diffusion thermoelectric power in the low-temperature range.

VII. CONCLUSIONS

We have measured the temperature dependence of the resistance of fluorine-intercalated graphite fibers as a function of fluorine concentration in C_xF fibers with x in the range $4.1<x<5.8$ Our results confirmed for the first time in a fibrous host material that a large concentration of fluorine (C_xF with $x\leq4.5$) leads to low-conductivity compounds. The room-temperature resistivity of these compounds is about a factor of 3–4 higher than what is observed on pristine vapor-grown graphite fibers heat treated at 2950 °C and is about 1 order of magnitude higher than the resistivity of more dilute C_xF compounds with $x\geq5.2$. At low temperature, each compound exhibits a logarithmic increase of resistivity with lowering temperature, though the magnitude of the effect is very sensitive to the fluorine concentration. Large negative magnetoresistance values were observed on the compound with the highest F concentration which were not found to originate from unintercalated regions. From magnetoresistance measurements, we found that the low-temperature dependence of the resistance can be explained as resulting from 2D carrier-carrier interaction effects and to a lesser extent to weak localization. At high temperature, all C_xF compounds show anomalous resistance behaviors which can perhaps be explained as resulting from a phase transition, in agreement with previous resistivity and thermal-expansion studies. Heat transport is almost entirely governed by lattice vibrations in the C_xF compound, in contrast with other low-stage acceptor GIC's, which exhibit a strong electronic contribution at low temperature. Also, our results clearly emphasize the low-temperature lattice thermal-conductivity enhancement associated with the intercalate. The temperature dependence of the thermoelectric power behaves in a way which is typical for stage-2 acceptor GIC's, indicating that low hole mobility rather than low charge density is responsible for the high resistivity.

ACKNOWLEDGMENTS

The authors are indebted to Professor J.-P. Michenaud for useful discussions and to Dr. M. Kinany-Alaoui for his cooperation in the experimental part of this work. The work performed in Louvain-la-Neuve was in the framework of the programme "Action de Recherche Concertée" sponsored by the Belgian State (Ministry of Scientific Policy). The work performed at the Massachusetts Institute of Technology (MIT) was supported by U. S. Air Force Office of Scientific Research (AFOSR) Contract No. F-49620-85-0147. L.P. acknowledges financial support from the Fonds National Belge de la Recherche Scientifique.

[1]D. Vaknin, I. Palchan, D. Davidov, H. Selig, and D. Moses, Synth. Met. **16**, 349 (1986).

[2]T. Mallouk, B. L. Hawkins, M. P. Conrad, K. Zilm, C. E. Magiel, and N. Bartlett, Philos. Trans. R. Soc. London Sect. A **314**, 179 (1985).

[3]T. Nakajima, B. Chang, T. Fujiwara, N. Watanabe, and M. Endo, Carbon **26**, 213 (1988).

[4]N. Watanabe, T. Nakajima, and H. Touhara, *Graphite Fluorides, Studies in Inorganic Chemistry* (Elsevier, Amsterdam, 1988), Vol. 8.

[5]M. S. Dresselhaus and G. Dresselhaus, Adv. Phys. **30**, 139 (1981).

[6]I. Ohana, I. Palchan, Y. Yacobi, D. Davidov, and H. Selig, Phys. Rev. B **38**, 12 627 (1988).

[7]L. Piraux, J. P. Issi, J. P. Michenaud, E. Mc Rae, and J.-F. Marêché, Solid State Commun. **56**, 576 (1985); L. Piraux, V. Bayot, J.-P. Michenaud, J.-P. Issi, E. McRae, and J.-F. Marêché, Solid State Commun. **59**, 711 (1986).

[8]L. Piraux, V. Bayot, X. Gonze, J.-P. Michenaud, and J.-P. Issi, Phys. Rev. B **36**, 9045 (1987).

[9]J. A. Woollam, V. Natarajan, and B. Brandt, Appl. Phys. Commun. **6**, 121 (1986).

[10]L. D. Woolf, H. Ikezi, and Y. R. Lin-Liu, Solid State Commun. **54**, 49 (1985).

[11]T. Enoki and J. T. Nicholls (private communication).

[12]L. Piraux, B. Nysten, J.-P. Issi, J.-F. Marêché, and E. McRae, Solid State Commun. **55**, 517 (1985); B. Nysten, L. Piraux, and J.-P. Issi, Synth. Met. **12**, 505 (1985); L. Piraux, B. Nysten, J.-P. Issi, L. Salamanca-Riba, and M. S. Dresselhaus, Solid State Commun. **58**, 265 (1986); L. Piraux, J.-P. Issi, J.-F. Marêché, and E. McRae, Synth. Met. **30**, 245 (1989).

[13]T. Nakajima, I. Kameda, N. Watanabe, and M. Endo, Carbon **24**, 343 (1985).

[14]T. Mallouk and N. Bartlett, J. Chem. Soc. Chem. Commun. **12**, 103 (1983).

[15]I. Palchan, D. Davidov, and H. Selig, J. Chem. Soc. Chem. Commun. **12**, 657 (1983).

[16]T. Nakajima, M. Kawaguchi, and N. Watanabe, Synth. Met. **7**, 117 (1983).

[17]T. Nakajima, T. Ino, N. Watanabe, and H. Takenaka, Carbon **26**, 397 (1988).

[18]L. Piraux, J.-P. Issi, and P. Coopmans, Measurement **5**, 2 (1987).

[19]M. S. Dresselhaus, G. Dresselhaus, K. Sugihara, I. L. Spain, and H. A. Goldberg, in *Graphite Fibers and Filaments,* Vol. 5 of *Springer Series in Materials Science,* edited by M. Cardona (Springer-Verlag, Berlin, 1988).

[20]H. Touhara, Y. Goto, N. Watanabe, K. Imaeda, T. Enoki, H. Inokuchi, and Y. Mizutani, Synth. Met. **23**, 467 (1988).

[21]G. Bergmann, Phys. Rev. B **28**, 2914 (1983).

[22]S. Hikami, A. I. Larkin, and Y. Nagaoka, Prog. Theor. Phys. **63**, 707 (1980).

[23]B. L. Altshuler, A. G. Aronov, and P. A. Lee. Phys. Rev. Lett. **44**, 1288 (1980); B. L. Altshuler, D. E. Khmelnitskii, A. I. Larkin, and P. A. Lee, Phys. Rev. B **22**, 5142 (1980); P. A. Lee and T. V. Ramakrishnan, *ibid.* **26**, 4009 (1982).

[24]H. Fukuyama, J. Phys. Soc. Jpn. **48**, 2169 (1980).

[25]M. Gijs, C. Van Haesendonck, and Y. Bruynseraede, J. Phys. F **16**, 1227 (1986).

[26]J. P. Issi and L. Piraux, Ann. Phys. (Paris) [Sér. 15E] **11**, 165 (1986).

[27]B. T. Kelly, Carbon **5**, 247 (1967); **6**, 71 (1968); **6**, 485 (1968).

[28]B. Poulaert, J. Heremans, J.-P. Issi, I. Zabala-Martinez, H. Mazurek, and M. S. Dresselhaus, in *Extended Abstracts of the 15th Biennial Carbon Conference,* edited by W. R. Forsman (American Carbon Society, Philadelphia, 1981), p. 92.

[29]M. Elzinga, D. T. Morelli, and C. Uher, Phys. Rev. B **26**, 3312 (1982).

[30]L. Piraux, M. Kinany-Alaoui, J.-P. Issi, A. Perignon, P. Pernot, and R. Vangelisti, Phys. Rev. B **38**, 4329 (1988).

[31]I. Ohana, I. Palchan, Y. Yacoby, D. Davidov, and H. Selig, Solid State Commun. **56**, 505 (1985).

[32]C. Castellani, C. Di Castro, M. Grilli, and G. Strinati, Phys. Rev. B **37**, 6663 (1988).

[33]C. S. Ting, A. Houghton, and J. R. Senna, Phys. Rev. B **25**, 1439 (1982).